PHYSICS BASED PROBABILISTIC SEISMIC HAZARD CALCULATIONS FOR SOUTHERN CALIFORNIA

R. Graves[1], S. Callaghan[2], E. Deelman[2], E. Field[3], N. Gupta[2], T. H. Jordan[2], G. Juve[2], C. Kesselman[2], P. Maechling[2], G. Mehta[2], D. Meyers[2], D. Okaya[2] and K. Vahi[2]

[1]*URS Corporation, 566 El Dorado St, Pasadena, CA 91101, USA*
[2]*University of Southern California, Los Angeles, CA, 90089, USA*
[3]*US Geological Survey, 525 S. Wilson Ave, Pasadena, CA, 91125, USA*
Email: robert_graves@urscorp.com

ABSTRACT:

Deterministic source and wave propagation effects such as rupture directivity and basin response can have a significant impact on near-fault ground motion levels, particularly at longer shaking periods. CyberShake, as part of the Southern California Earthquake Center's (SCEC) Community Modeling Environment, is developing a methodology that explicitly incorporates these effects within seismic hazard calculations through the use of physics-based 3D ground motion simulations. To calculate a waveform-based probabilistic hazard curve for a site of interest, we begin with Uniform California Earthquake Rupture Forecast, Version 2 (UCERF2) and identify all ruptures (excluding background seismicity) within 200 km of the site of interest. We convert the UCERF2 rupture definition into multiple rupture variations with differing hypocenter location and slip distribution, which results in about 400,000 rupture variations per site. Strain Green Tensors are calculated for the site of interest using the SCEC Community Velocity Model, Version 4 (CVM4), and then, using reciprocity, we calculate synthetic seismograms for each rupture variation. Peak intensity measures (e.g., spectral acceleration) are then extracted from these synthetics and combined with the original rupture probabilities to produce probabilistic seismic hazard curves for the site. Thus far, we have produced hazard curves for spectral acceleration at a suite of periods ranging from 3 to 10 seconds at about 20 sites in the Los Angeles region, with the ultimate goal being the production of full hazard maps. Our results indicate that the combination of rupture directivity and basin response effects can lead to an increase in the hazard level for some sites, relative to that given by a conventional Ground Motion Prediction Equation (GMPE). Additionally, and perhaps more importantly, we find that the physics-based hazard results are much more sensitive to the assumed magnitude-area relations and magnitude uncertainty estimates used in the definition of the ruptures than is found in the traditional GMPE approach. This reinforces the need for continued development of a better understanding of earthquake source characterization and the constitutive relations that govern the earthquake rupture process.

KEYWORDS: ground motion simulation, probabilistic seismic hazard, earthquake rupture characterization

1. INTRODUCTION

Probabilistic Seismic Hazard Analysis (PSHA) provides a framework for quantifying the expectation of exceeding a particular ground motion level at a particular site within a specified time interval. The basic methodology was originally proposed by Cornell (1968) and has found wide acceptance in many earthquake engineering applications over the last four decades. The two main inputs to the PSHA are the characterization of potential earthquake sources and the estimation of ground motion levels associated with these sources. Source characterization consists of the definition of sources or faults (e.g., location, length, width, geometry) and their level of activity (e.g. slip rate, average recurrence interval, characteristic magnitude). Estimation of ground motion levels is traditionally done using a Ground Motion Prediction Equation (GMPE) and consists of determining the conditional probability of exceeding a target ground motion level (e.g., 0.2 g PGA) at a particular

site for each of the sources being considered. By combining the conditional ground motion exceedance probabilities with the probability of rupture for each of the prescribed sources, and then integrating over all sources, one can develop a full hazard curve. Since the process deals with probabilities, a key component of both sets of inputs is the quantification of uncertainties associated with the various parameters.

To estimate the ground motion levels in CyberShake, we replace the GMPE with a full 3D waveform simulation of the ground motions for each rupture scenario. While this allows us to explicitly account for deterministic aspects of source rupture and wave propagation, it entails a significant computational burden and also requires some modification to the way in which the ruptures are specified. This is because the GMPE implicitly incorporates source and path variability through its uncertainty, commonly referred to as "sigma". However, for CyberShake, we must estimate this uncertainty by considering multiple scenarios (e.g. slip distributions, hypocenter locations, etc.) for each earthquake source. UCERF2 (Field et al, 2008) has about 10,000 defined ruptures of magnitude 6 and larger, however, in the current phase of CyberShake, this translates into roughly 400,000 rupture scenarios for which we must simulate ground motions. To make this computationally feasible, we utilize reciprocity and calculate 3D Strain Green Tensors for each site, which are then used to simulate the ground motions for each rupture scenario using the representation theorem. The entire process has been automated using computational workflows and relies on the resources of the SCEC Community Modeling Environment and various TeraGrid computational facilities (Jordan and Maechling, 2003, Deelman et al, 2006).

Figure 1 shows a map of the Southern California region where CyberShake is currently being implemented. The first set of 10 sites (red squares) has been completed, and the additional sites are currently in progress. The goal for early 2009 is to cover the greater Los Angeles basin region with a grid of sites having an average spacing of about 5 km. This will provide a basis for generating full hazard maps of this region.

2. EARTHQUAKE RUPTURE CHARACTERIZATION

UCERF2 utilizes the rectangularized fault definitions given by the SCEC Community Fault Model version 3.0 (CFM3). Magnitudes for ruptures of these faults are estimated using magnitude-area scaling relations. Four scaling relations are currently implemented within UCERF2; Ellsworth-B (WGCEP, 2003), Hanks and Bakun (2007), Somerville et al (2006) and Wells and Coppersmith (1994); although currently only Ellsworth-B and Hanks-Bakun are given non-zero weights. For magnitudes larger than about 7, the Ellsworth-B and Hanks-Bakun relations predict magnitudes about 0.2 units larger for the same fault area compared to Somerville and Wells-Coppersmith. While this has little impact on calculations utilizing GMPEs, we have found that this has a significant impact on physics-based simulations. The 0.2 unit increase in magnitude corresponds to a factor of 2 increase in seismic moment. At long periods and for a fixed fault area, the numerical simulations scale almost directly with increasing seismic moment (M_o). However, the GMPE has a built-in magnitude-area relation that implicitly adjusts the area for the prescribed magnitude. Thus, the ground motions for the empirical model scale more like $M_o^{1/3}$ as the magnitude is changed.

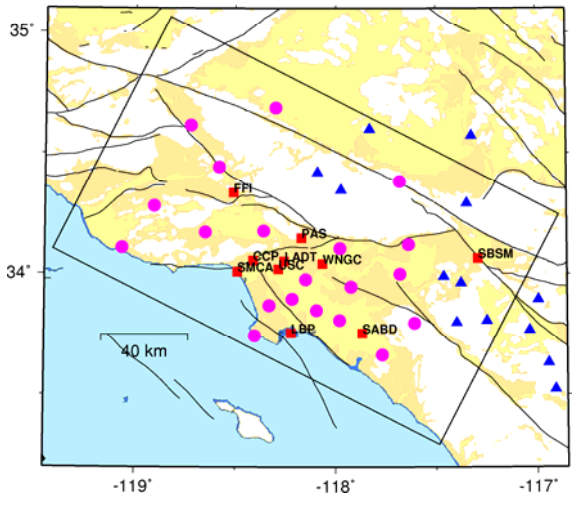

Figure 1: Map of Southern California showing target region for CyberShake. Red squares indicate 10 original sites, magenta circles and blue triangles are sites currently being computed. Eventually, the entire rectangular region will be covered by a grid of sites allowing for the generation of hazard maps.

For this reason, it is imperative that we specify the

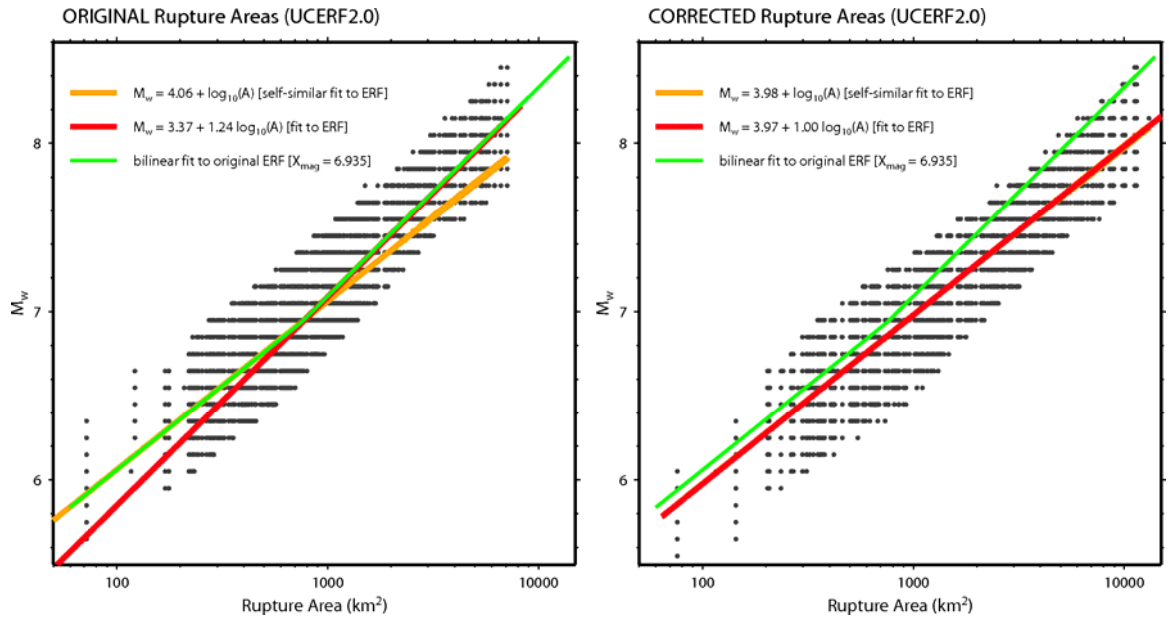

Figure 2: Magnitude vs area plots for all UCERF2 ruptures. Left panel shows original rupture set based on the Ellsworth-B and Hanks-Bakun scaling relations. Right panel shows corrected rupture set based on Somerville scaling relation. Lines are regression fits through the roughly 10,000 data points.

fault areas and magnitudes for CyberShake using the most appropriate scaling relation. The Somerville relation is based on fault rupture characterizations that were developed using waveform inversions of well recorded earthquakes. These inversions utilize the same wave propagation physics and ground motion representation theorems as implemented in CyberShake. Thus, for consistency in the CyberShake implementation, we have modified the weighting of the scaling relations in UCERF2 to give full weight to Somerville. In doing this, we retained the magnitude estimates given by the original UCERF2 definitions, and simply adjusted the fault areas (by increasing their down-dip widths) such that the resulting set of ruptures correspond, on average, to the Somerville relation. Figure 2 plots all the UCERF2 ruptures for the original and corrected areas.

In order to perform the numerical simulations, we need to develop a full kinematic description of fault rupture for each scenario. This includes slip distribution, hypocenter location, rupture propagation and slip time function. For a given fault and Mw, the rupture model is generated in the wavenumber domain by constraining the amplitude spectrum of slip to fit a K^{-2} falloff (Somerville et al, 1999; Mai and Beroza, 2002). The slip velocity function is constructed using two triangles as shown in Figure 3, with the rise time scaling with increasing magnitude (Somerville et al., 1999). For each fault, multiple hypocenters and slip distributions are considered. Hypocenters are placed every 20 km along strike and two slip distributions are run for each hypocenter. The current implementation only considers

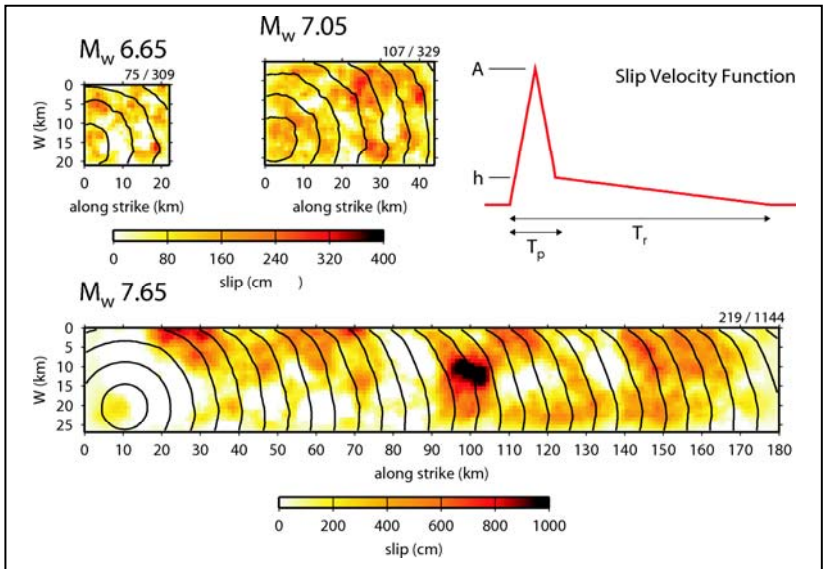

Figure 3: Kinematic rupture models for scenarios of magnitude 6.65, 7.05 and 7.65. Cotours of rupture time are shown at 2 second intervals for each rupture. Upper right displays schematic view of slip velocity function used for the kinematic description.

median values for rise time and rupture velocity (80% of local Vs). Figure 3 displays representative rupture models for 3 different magnitudes.

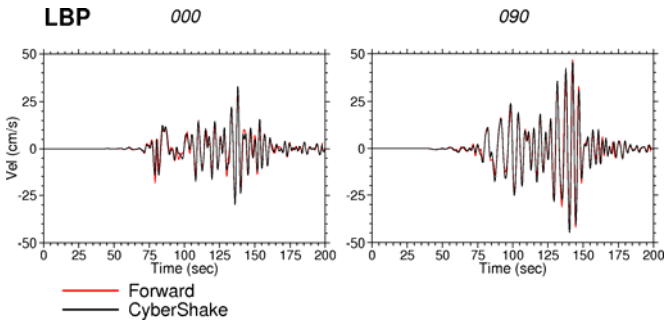

Figure 4: Comparison of waveforms simulated at Long Beach for a M_w 7.8 rupture of the San Andreas fault using a forward calculation (red) and the reciprocal SGT method of CyberShake (black). The bandwidth of the motions is f < 0.5 Hz.

3. VERIFICATION

For each site of interest, we first compute a full set of SGTs for all ruptures within 200 km of the site. The SGTs are calculated via reciprocity within the prescribed 3D velocity structure using a parallelized anelastic FD algorithm (Graves, 1996; Graves and Wald, 2001). We set the minimum shear wave velocity at 500 m/s and using a grid spacing of 200 m we obtain a maximum frequency resolution of 0.5 Hz. Two calculations are required, one each to obtain the SGTs for each of the two orthogonal horizontal components of motion. Each fault rupture surface is sampled at a 1 km spacing, and the SGTs are saved for each of these fault surface locations. In total, there are about 420,000 SGT locations, and the resulting set of SGTs requires about 20 GB of storage for each site.

The advantage of pre-computing and saving the SGTs is that it requires only two large-scale 3D simulations per site (roughly 10 hours per simulation using 200 CPUs). Once computed, the convolution of the SGTs with each of the approximately 400,000 ruptures is quite fast and easily parallelizable (about 24 hours total runtime for all ruptures). Running a forward simulation for each rupture would have the advantage of providing ground motions for a great number of locations, but this approach would not be currently practical for the large number of rupture scenarios that need to be considered. Theoretically, these two approaches produce exactly the same results. Figure 4 compares ground motions simulated at a site in Long Beach (LBP) for a Mw 7.8 rupture of the San Andreas fault using both approaches. The agreement between the two calculations is excellent, with the very slight differences in this case due to small differences in the spatial discretization of the forward and reciprocal models.

The bulk of recorded strong motion data are from events of magnitude from about 6 to 7 and for distances out to about 70 km. Within these ranges, the GMPEs are quite well constrained. Figure 5 compares CyberShake simulations at Pasadena (PAS) against GMPE

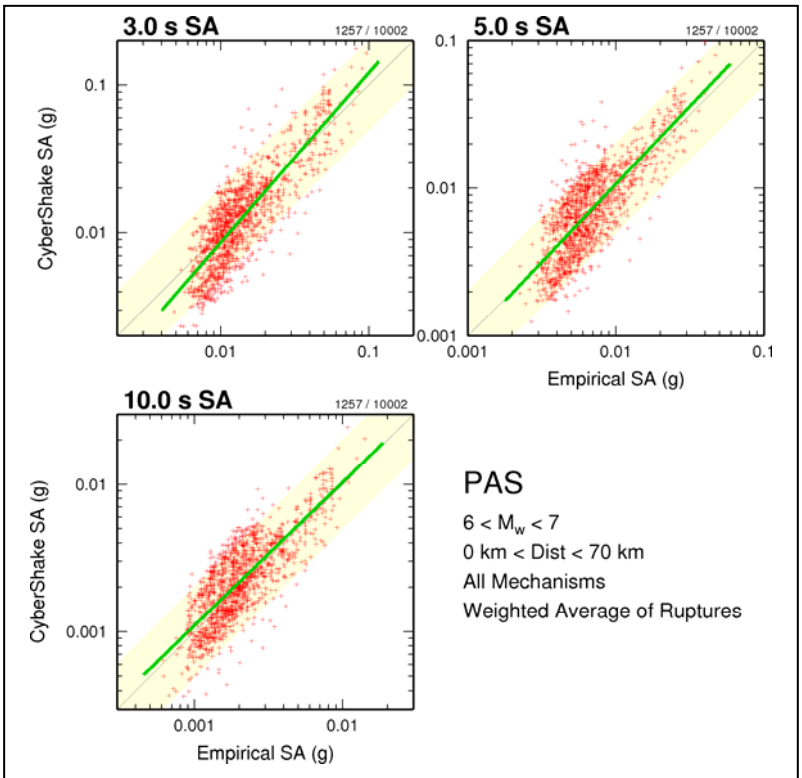

Figure 5: Comparison of CyberShake computed motions with empirical estimates at Pasadena for the subset of ruptures having magnitudes between 6 and 7, and within 70 km closest distance to the site. The emipircal estimates are the average of the four GMPEs discussed in the text. The three panels show spectral accelearation at oscillator periods of 3 sec (upper left), 5 sec (upper right), and 10 sec (lower left). The green line in each panel is a least squares fit to the points.

predictions for the subset of UCERF2 rupture scenarios within this magnitude and distance range. For this comparison, we have averaged the results of four recent GMPEs; Abrhamson and Silva (2008), Boore and Atkinson (2008), Campbell and Bozorgnia (2008), and Chiou and Youngs (2008). On average, the agreement between the CyberShake and empirical predictions is quite good and supports the validity of the CyberShake approach. In computing the CyberShake values, we have averaged over all hypocenters and slipmodels for a given source. Thus, the scatter of these results is due primarily to the magnitude (i.e., static stress drop) variability of the sources as defined by UCERF2. Additionally, the scatter is not isotropic, but is skewed vertically along the CyberShake axis indicating that the magnitude variability produces a much greater effect on the CyberShake ground motions than on the GMPE ground motions. These results also support the adjustment of fault rupture areas described in the previous section. If we had used the original UCERF2 areas, which on average are smaller by about 25% for these magnitudes, then our kinematic rupture models would require an increase in average slip of a comparable amount. The resulting CyberShake simulations would then be about 25% higher on average, which would not be consistent with the GMPE predictions.

4. HAZARD CURVES

Figure 6 compares 3 second Spectral Acceleration (SA) hazard curves computed at four sites with the CyberShake Platform against standard curves derived from the GMPEs of Boore and Atkinson (2008) and Campbell and Bozorgnia (2008). Background seismicity is excluded from both models and the GMPE calculation is truncated at 3 sigma. Both GMPEs utilize V_{s30} (the average shear wave velocity in the upper 30 meters) to account for site response effects. Additionally, the Campbell-Bozorgnia relation incorporates a basin response effect based on the depth to Vs =2.5 km/s beneath the site (referred to as Z2.5). Rupture directivity effects are not explicitly included in these GMPEs. However, all of these effects are naturally included in the CyberShake results through the use of the 3D velocity structure for the ground motion simulations. The hazard curves were generated using the resources and applications of OpenSHA (Field et al., 2003, www.opensha.org).

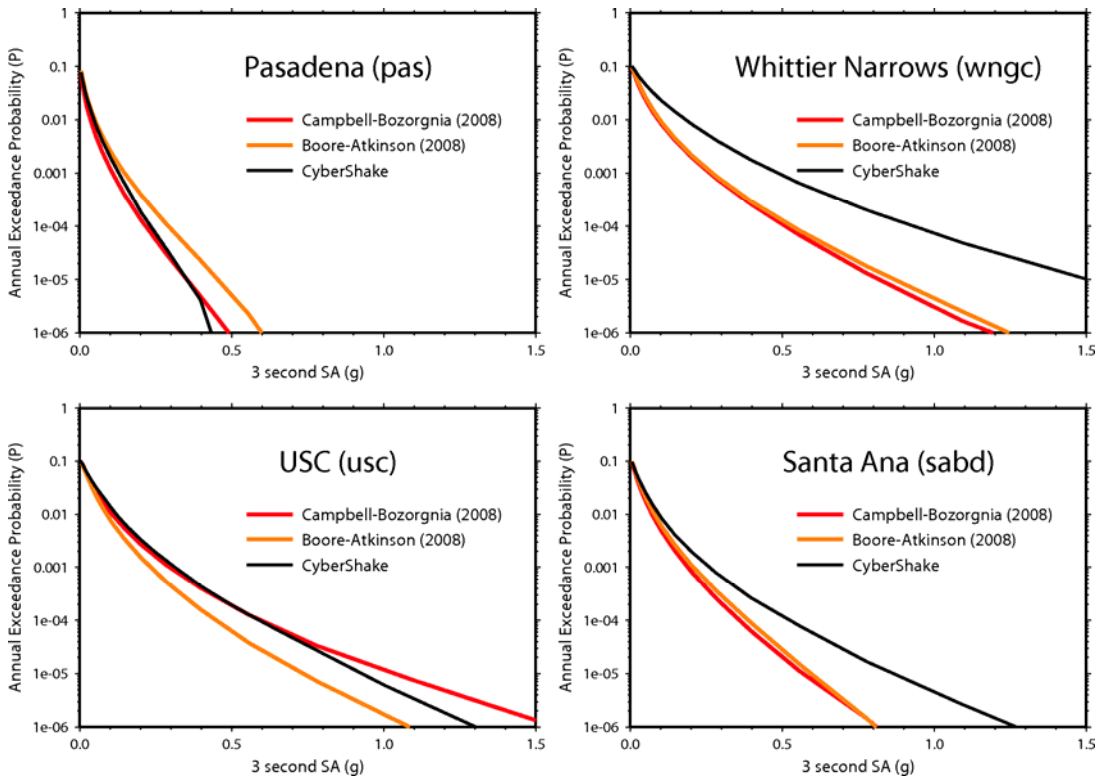

Figure 6: Hazard curves for spectral acceleration (SA) at 3 sec period at four Los Angeles region sites for all ruptures of Mw 6 and greater excluding background seismicity. The empirical models use a truncation at 3 sigma.

Table 1 lists the site-specific parameters used for each location. The PAS site can be regarded as a "rock" site, whereas the USC, WNGC and SABD sites are "basin" sites located on a thick accumulation of soft sediments.

Table 1. Site parameters used for hazard computations.

Site	LON.	LAT.	Vs30 (m/s)	Z2.5 (km)
PAS	-118.1712	34.1484	760	0.34
USC	-118.2860	34.0192	270	4.06
WNGC	-118.0653	34.0418	270	2.93
SABD	-117.8678	33.7541	270	2.57

At the rock site (PAS), both the CyberShake and GMPE approaches produce similar results, whereas for the basin sites, the hazard levels produced by CyberShake are generally higher than the GMPE results. We infer the higher CyberShake hazard levels result from a combination of rupture directivity and basin response effects that are not fully included in the empirical models. This is particularly evident for the WNGC and SABD sites which have modest basin depths, but still exhibit relatively high ground motion hazard from the numerical simulations. Previous TeraShake (Olsen et al., 2006 and 2008) and ShakeOut (Graves, 2008) ground motion modeling studies have shown that these sites are susceptible to channeling and amplification of basin waves for larger rupture on the southern San Andreas fault. This amplification effect represents a coupling of rupture directivity and basin response which cannot be accounted for using the existing GMPE parameterizations.

5. DISAGGREGATION

Disaggregation breaks down the hazard to find which sources most significantly contribute to the hazard at a particular site. Disaggregation can be done on probability or ground motion level. Figure 7 shows the magnitude/distance disaggregation of the Campbell-Bozorgnia 3 sec SA hazard curve at a ground motion level of 0.284 g for the SABD site. The results are plotted as a function of magnitude, distance and percent contribution to the hazard. It turns out that for all sites in the Los Angeles basin region, the pattern of the disaggregations is similar for both the empirical and CyberShake results. This occurs because the overall hazard for sites within the Los Angeles region is typically controlled by nearby moderate-sized (M_w 6-7) events and more distant large magnitude events (M_w > 7.5) on the San Andreas fault. The fact that CyberShake reproduces this pattern is a key validation of the methodology. The main differences between CyberShake and the empirical results are 1) the contribution percentages and 2) the probability of exceedance (P). We believe these differences are real, and result from the explicit inclusion of deterministic source rupture and wave propagation effects within the CyberShake methodology.

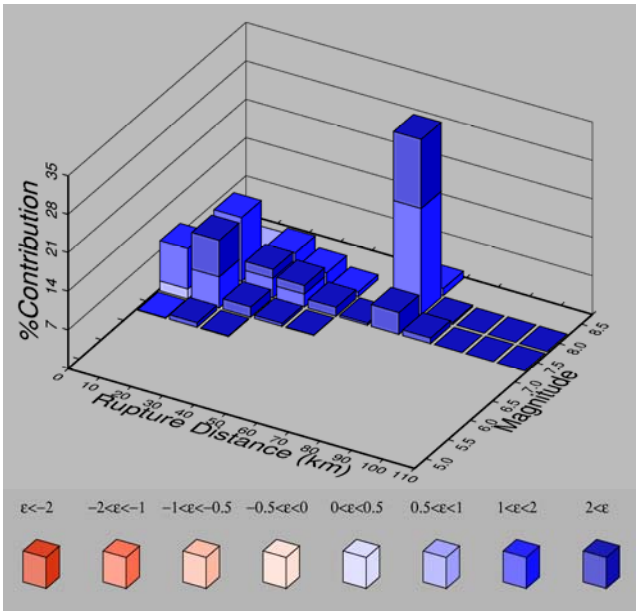

Figure 7: Magnitude/distance disaggregation at SABD for 3 sec SA at a ground motion level of 0.284 g. Hazard results are based on the GMPE of Campblee-Bozorgnia.

6. CONCLUSIONS

The SCEC CyberShake project has developed an approach for implementing physics-based waveform simulations in PSHA calculations. The advantage of the physics-based approach over the GMPE approach is that deterministic earthquake rupture and wave propagation effects are explicitly include in the ground motion response. The process requires significant computational resources which have been made available through the SCEC Community

Modeling Environment (www.scec.org/cme). Our preliminary results demonstrate this approach is viable, and we are working toward developing hazard maps for the Southern California region by early 2009.

Incorporation of physics-based ground motions within the PSHA framework requires careful consideration of how the earthquake ruptures are characterized. The current UCERF2 characterization uses an average of two magnitude-area scaling relations (Ellsworth-B and Hanks-Bakun), which systematically under-estimate fault areas compared with physics-based rupture model inversions for event magnitudes larger than about 6.7, particularly for strike-slip faults (Somerville, 2006). This has little consequence on the traditional GMPE based hazard calculations because the GMPEs do not explicitly consider fault rupture area (or static stress drop) in determining ground motion levels. However, the physics based approach is quite sensitive to the magnitude-area scaling because both magnitude and rupture area are required to fully characterize the rupture. Thus, using a fault area that is too small requires a corresponding increase in slip to preserve the target magnitude (seismic moment) in the physics-based simulations, which scales almost directly into ground motion amplitude at the longer periods. To circumvent this problem, we have modified the original UCERF2 fault descriptions by extending their down-dip widths such that the resulting fault rupture areas correspond, on average, to the Somerville (2006) scaling relation. Validation tests indicate that the modified rupture descriptions provide a much better match to recorded ground motion levels than the original descriptions.

Magnitude variability for the characteristic ruptures in UCERF2 is about 0.7 units or larger for a given fault rupture area. Since the fault rupture area is held fixed in these characteristic ruptures, the average ground motion levels in the numerical simulations scale almost directly with seismic moment. This 0.7 unit magnitude range corresponds to a change in seismic moment of over a factor of 10. However, rupture area is not a parameter used by the GMPEs. Thus, the GMPE implicitly adjusts the area (to maintain a constant median static stress drop) when the magnitude is changed, and consequently the ground motion levels predicted from the GMPEs are much less sensitive to changes in magnitude, scaling roughly with seismic moment to the one-third power. The magnitude range of 0.7 units produces only about a factor of two variability in the median ground motion levels predicted by the GMPEs. This raises two important issues with respect to magnitude characterization. First, the strong sensitivity of the numerical simulation results to magnitude variability for a constant rupture area (combined with the relative lack thereof for the GMPEs), suggests that the prescribed range of magnitude variability defined by UCERF2 needs to be examined very carefully. Second, it is possible that the large range of UCERF2 magnitude variability coupled with the use of GMPEs actually double counts this effect due to its incorporation within the uncertainty estimates (sigma) of the GMPE.

ACKNOWLEDGEMENTS

Funding for this work was provided by SCEC under NSF grants EAR-0623704 and OCI-0749313. The large-scale simulations were run at USC's Center for High Performance Computing and Communications (http://www.usc.edu/hpcc) and NSF's TeraGrid (www.teragrid.org) under agreement with the SCEC CME project.

REFERENCES

Abrahamson, N.A. and Silva, W.J. (2008). Summary of the Abrahamson and Silva NGA ground motion relations. *Earthquake Spectra* **24(S1),** accepted for publication.

Boore, D.M. and Atkinson, G.M. (2008). Ground motion prediction equations for the average horizontal component of PGA, PGV, and 5%-damped PSA at spectral periods between 0.01 and 10.0 s. *Earthquake Spectra* **24(S1),** accepted for publication.

Campbell, K.W. and Bozorgnia, Y. (2008). NGA ground motion model for the geometric mean horizontal component of PGA, PGV, PGD, and 5%-damped linear elastic response spectra for periods ranging from 0.01 to 10 s. *Earthquake Spectra* **24(S1),** accepted for publication.

Chiou, B.S.-J. and Youngs, R.R. (2008). Chiou and Youngs PEER-NGA empirical ground motion model for the average horizontal component of peak acceleration and pseudo-spectral acceleration for spectral periods of 0.01 to 10 seconds *Earthquake Spectra* **24(S1),** accepted for publication.

Cornell, C., (1968). Engineering seismic risk analysis, *Bull. Seismol. Soc. Am.;* **58**, 1583-1606.

Deelman, E., S. Callaghan, E. Field, H. Francoeur, R. Graves, N. Gupta, V. Gupta, T. H. Jordan, C. Kesselman, P. Maechling, J. Mehringer, G. Mehta, D. Okaya, K. Vahi, Li. Zhao (2006). Managing Large-Scale Workflow Execution from Resource Provisioning to Provenance tracking: The CyberShake Example, *2nd International Conference on e-Science and Grid Computing*, Amsterdam.

Field, E.H., T.H. Jordan, and C.A. Cornell (2003). OpenSHA: A developing Community-Modeling Environment for Seismic Hazard Analysis, *Seismological Research Letters*, **74**, 406-419.

Field, E. H., T. E. Dawson, K. R. Felzer, A. D. Frankel, V. Gupta, T. H. Jordan, T. Parsons, M. D. Petersen, R. S. Stein, R. J. Weldon II, and C. J. Wills (2008). The Uniform California Earthquake Rupture Forecast, Version 2 (UCERF 2), *USGS Open File Report 2007-1437*.

Graves, R., (1996). Simulating seismic wave propagation in 3D elastic media using staggered grid finite differences, *Bull. Seismol. Soc. Am.,* **86**, 1091–1106.

Graves, R., B. Aagaard, K. Hudnut, L. Star, J. Stewart, and T. H. Jordan (2008). Broadband simulations for M_w 7.8 southern San Andreas Earthquakes: Ground motion sensitivity to supture speed, *submitted to Geophys. Res. Lett.*

Graves, R. W. and D. J. Wald (2001). Resolution analysis of finite fault source inversion using 1D and 3D Green's functions, Part 1: Strong Motions, *J. Geophys. Res.*, **106**, 8745-8766.

Hanks, T. C., and W. H. Bakun (2007). *M*-log *A* observations for recent large earthquakes, *Bull. Seismol. Soc. Am.*, in press.

Jordan, T. H., and P. Maechling, (2003). The SCEC Community Modeling Environment—an information infrastructure for system-level earthquake science, *Seismol. Res. Lett.*, **74**, 324-328.

Mai, M., and G. Beroza, (2002). A spatial random field model to characterize complexity in earthquake slip, *J. Geophys., Res.*, **107**, B11.

Olsen, K., S. Day, J. Minster, Y. Cui, A. Chourasia, M. Faerman, R. Moore, P. Maechlin, and T. Jordan, (2006). Strong shaking in Los Angeles expected from a southern San Andreas earthquake, *Geophys. Res. Lett.*, **33**, L07305.

Olsen, K. B., S. M. Day, J. B. Minster, Y. Cui, A Chouasia, R. Moore, P. Maechling, and T. Jordan, (2008). TeraShake2: simulation of M_w 7.7 earthquakes on the southern San Andreas fault with spontaneous rupture description, *Bull. Seismol. Soc. Am.*, in press.

Somerville, P., K. Irikura, R. Graves, S. Sawada, D. Wald, N. Abrahamson, Y. Iwasaki, T. Kagawa, N. Smith, and A. Kowada, (1999). Characterizing crustal earthquake slip models for the prediction of strong ground motion, *Seismol. Res. Lett.*, **70**, 199–222.

Somerville, P. (2006). Review of magnitude-area scaling of crustal earthquakes, *Report to 2007 WGCEP*, URS Corp., Pasadena, CA, 22 pp.

Wells, D. L., and K. J. Coppersmith (1994). New empirical relationships among magnitude, rupture length, rupture width, rupture area, and surface displacement, *Bull. Seismol. Soc. Am.*, **84**, 974- 1002.

Working Group on California Earthquake Probabilities (2003). Earthquake Probabilities in the San Francisco Bay Region: 2002–2031, *USGS Open-File Report 2003-214*.